PROCEEDINGS OF SCIENCE

Hadroproduction of open heavy flavour for PDF analyses

Ilkka Helenius
University of Jyvaskyla, Department of Physics, P.O. Box 35, FI-40014 University of Jyvaskyla, Finland
Helsinki Institute of Physics, P.O. Box 64, FI-00014 University of Helsinki, Finland
Institute for Theoretical Physics, Tübingen University, Auf der Morgenstelle 14, 72076 Tübingen, Germany
E-mail: ilkka.m.helenius@jyu.fi

Hannu Paukkunen*
University of Jyvaskyla, Department of Physics, P.O. Box 35, FI-40014 University of Jyvaskyla, Finland
Helsinki Institute of Physics, P.O. Box 64, FI-00014 University of Helsinki, Finland
E-mail: hannu.paukkunen@jyu.fi

Due to the large masses of the charm and bottom quarks, their production cross sections are calculable within the perturbative QCD. This makes the heavy-quark mesons important observables in high-energy collisions of protons and nuclei. However, the available calculations for heavy-flavored-meson hadroproduction have been somewhat problematic in reliably describing the cross sections across the full kinematic range from zero to very high p_{T}. This has put some question marks on the robustness of LHC heavy-flavored-meson measurements in studying the partonic structure of the colliding hadrons and nuclei. Here, we introduce SACOT-m_{T} – a novel scheme for open heavy-flavour hadroproduction within the general-mass variable-flavour-number formalism that solves this problem. The introduced scheme is an analogue of the SACOT-χ scheme often used for deeply-inelastic scattering in global analyses of PDFs.

XXVII International Workshop on Deep-Inelastic Scattering and Related Subjects - DIS2019
8-12 April, 2019
Torino, Italy

*Speaker.

PoS(DIS2019)160

1. Introduction

The hadroproduction of open heavy flavour – D mesons in particular – has recently been advocated as a promising constraint for proton parton distribution functions (PDFs) [1, 2]. The theoretical description is typically based on the fixed flavour-number scheme (FFNS) [3], FONLL code [4], or FFNS matched to parton showers [5]. However, the use of e.g. FFNS calculation in conjunction with PDFs defined in variable flavour-number schemes (the commonly used general-purpose PDFs) may be too restrictive, and in this sense calculations within the framework of general-mass variable-flavour-number scheme (GM-VFNS) would be more natural. Here, we will discuss our novel implementation of the GM-VFNS, the so-called SACOT-$m_{\rm T}$ scheme [6].

2. D-meson production in fixed flavour-number scheme

Within FFNS – assuming no intrinsic heavy-quark content in the proton – the massive quarks Q are always produced in pairs by the partonic processes, $g+g \rightarrow Q\overline{Q}+X$, $q+\overline{q} \rightarrow Q\overline{Q}+X$, $q+g \rightarrow Q\overline{Q}+X$. The cross section for inclusive Q production can be written as an integral of PDFs $f_i^p(x_1,\mu^2_{\rm fact})$ and partonic cross sections $d\hat{\sigma}^{ij}$,

$$\frac{d\sigma(p+p\rightarrow Q+X)}{dp_{\rm T}dy} = \sum_{ij}\int dx_1 dx_2 f_i^p(x_1,\mu^2_{\rm fact})\frac{d\hat{\sigma}^{ij\rightarrow Q+X}(\tau_1,\tau_2,m^2,\mu^2_{\rm ren},\mu^2_{\rm fact})}{dp_{\rm T}dy} f_j^p(x_2,\mu^2_{\rm fact}),$$

where y and $p_{\rm T}$ denote the rapidity and transverse momentum of the produced heavy quark. The factorization and renormalization scales are marked by $\mu^2_{\rm fact}$ and $\mu^2_{\rm ren}$. The kinematic variables $\tau_{1,2}$ are the "massive" Mandelstam variables,

$$\tau_1 \equiv p_1\cdot p_3/p_1\cdot p_2 = m_{\rm T}e^{-y}/(\sqrt{s}x_2), \quad \tau_2 \equiv p_2\cdot p_3/p_1\cdot p_2 = m_{\rm T}e^{y}/(\sqrt{s}x_1), \quad m^2_{\rm T} = p^2_{\rm T}+m^2,$$

denoting the momenta of the incoming partons and outgoing heavy quark by $p_{1,2}$ and p_3, respectively. The partonic cross sections scale as $d\hat{\sigma}^{ij\rightarrow Q+X} \sim \tau_{1,2}^{-n}$, and, thanks to the heavy-quark mass, remain finite even at $p_{\rm T}=0$. The heavy-quark cross sections can be turned into, say D^0-meson production cross sections by folding with $Q\rightarrow \mathrm{D}^0$ fragmentation functions (FFs) $D_{Q\rightarrow \mathrm{D}^0}(z)$. The fragmentation variable z is not unique when the masses of the heavy quark and D^0 meson are kept non zero. For simplicity, we define $z\equiv E_{\mathrm{D}^0}/E_Q$, where E_{D^0} and E_Q are the energies of the D^0 meson and heavy quark in the center-of-mass frame of the p-p collision. Assuming that the fragmentation is collinear we get,

$$\frac{d\sigma(p+p\rightarrow \mathrm{D}^0+X)}{dP_{\rm T}dY} = \sum_{ij}\int \frac{dz}{z} dx_1 dx_2 f_i^p(x_1,\mu^2_{\rm fact})\frac{d\hat{\sigma}^{ij\rightarrow Q+X}}{dp_{\rm T}dy} f_j^p(x_2,\mu^2_{\rm fact}) D_{Q\rightarrow \mathrm{D}^0}(z),$$

where the (lower case) partonic and (upper case) hadronic variables are related by

$$p^2_{\rm T} = \frac{M^2_{\rm T}\cosh^2 Y - z^2m^2}{z^2}\left(1+\frac{M^2_{\rm T}\sinh^2 Y}{P^2_{\rm T}}\right)^{-1} \xrightarrow{P_{\rm T}\rightarrow\infty} \left(\frac{P_{\rm T}}{z}\right)^2,$$
$$y = \sinh^{-1}\left(\frac{M_{\rm T}\sinh Y}{P_{\rm T}}\frac{p_{\rm T}}{m_{\rm T}}\right) \xrightarrow{P_{\rm T}\rightarrow\infty} Y,$$

and $M_{\rm T}=\sqrt{P^2_{\rm T}+M^2_Q}$ marks the hadronic transverse mass. While this framework appears to work well at low $P_{\rm T}$ (see e.g. [7]), the description seems to deteriorate towards high $P_{\rm T}$. Presumably, this can be attributed to the $\log(p^2_{\rm T}/m^2)$ behaviour of the partonic cross sections which begin to dominate and should be resummed, as we will come to conlcude.

PoS(DIS2019)160

3. D-meson production in general-mass variable-flavour-number scheme

The GM-VFNS description can be obtained from FFNS by resumming the $\log(p_{\mathrm{T}}^2/m^2)$ terms that appear in FFNS. As an example, in Figure 1 the diagram (a) gives rise to such logarithmic behaviour when the initial-state gluon splits into a $Q\overline{Q}$ pair. This is only the first of the whole series of diagrams that are in GM-VFNS summed into the heavy-quark PDF f_Q^p. Effectively, this

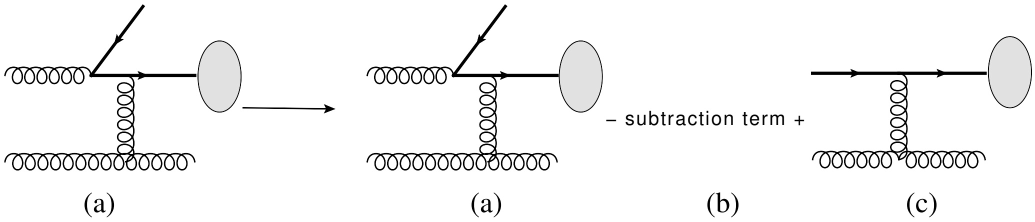

Figure 1: Origin of the heavy-quark initiated subprocess illustrated.

summation can be realized by including the heavy-quark initiated contribution (c) and a subtraction term (b) that avoids the double counting between diagrams (a) and (c). The contribution from $Qg \to Q+X$ channel, represented here by the diagram (c), can be written as

$$\int \frac{dz}{z} dx_1 dx_2\, f_Q^p(x_1, \mu_{\mathrm{fact}}^2) \frac{d\hat{\sigma}^{Qg\to Q+X}(\tau_1,\tau_2)}{dp_{\mathrm{T}}dy} f_g^p(x_2, \mu_{\mathrm{fact}}^2) D_{Q\to \mathrm{D}^0}(z)\,.$$

The subtraction term (b) is obtained from this same expression by replacing the heavy-quark PDF with its perturbative expression,

$$f_Q^p(x, \mu_{\mathrm{fact}}^2) = \left(\frac{\alpha_s}{2\pi}\right) \log\left(\frac{\mu_{\mathrm{fact}}^2}{m^2}\right) \int_x^1 \frac{\mathrm{d}\ell}{\ell} P_{qg}\left(\frac{x}{\ell}\right) f_g^p(\ell, \mu_{\mathrm{fact}}^2) + \mathcal{O}(\alpha_s^2)\,,$$

where α_s is the QCD coupling, and P_{qg} is the usual gluon-to-quark splitting function. However, the exact form of $d\hat{\sigma}^{Qg\to Q+X}(\tau_1,\tau_2)$ in the above expressions is not unique [8]. In practice, we can only require that the zero-mass $\overline{\mathrm{MS}}$ expressions are recovered at high p_{T},

$$\frac{d\hat{\sigma}^{Qg\to Q+X}(\tau_1,\tau_2)}{dp_{\mathrm{T}}dy} \xrightarrow{p_{\mathrm{T}}\to\infty} \frac{d\hat{\sigma}^{qg\to q+X}(\tau_1^0,\tau_2^0)}{dp_{\mathrm{T}}dy}\,, \qquad \tau_{1,2}^0 = \tau_{1,2} \xrightarrow{m\to 0} p_{\mathrm{T}} e^{\mp y}/(\sqrt{s}x_{2,1})\,.$$

The easiest option is to define $d\hat{\sigma}^{Qg\to Q+X}(\tau_1,\tau_2) \equiv d\hat{\sigma}^{qg\to q+X}(\tau_1^0,\tau_2^0)$, i.e. use the zero-mass expressions to begin with. This is known as the SACOT scheme [9]. The problem of this choice is that it leads to infinite cross sections towards $P_{\mathrm{T}} \to 0$ due to the $d\hat{\sigma}^{qg\to q+X}/d^3p \sim (\tau_{1,2}^0)^{-n}$ behaviour of the partonic cross sections. In the so-called FONLL scheme [4] this is avoided by multiplying the partonic cross section by an ad-hoc damping factor $p_{\mathrm{T}}^2/(p_{\mathrm{T}}^2+c^2m^2)$ with $c \sim 5$, which serves to tame the unphysical behaviour at small p_{T}. Alternatively, the problematic behaviour can be avoided simply by retaining the kinematics of the $Q\overline{Q}$-pair production which, deep down, is the underlying process we describe. With this physical picture in mind, we define $d\hat{\sigma}^{Qg\to Q+X}(\tau_1,\tau_2) \equiv d\hat{\sigma}^{qg\to q+X}(\tau_1,\tau_2)$ taking $\tau_{1,2} = m_{\mathrm{T}} e^{\mp y}/(\sqrt{s}x_{2,1})$ as in FFNS. This leads to well-behaved cross sections in the $P_{\mathrm{T}} \to 0$ limit. We call this the SACOT-m_{T} scheme, as it shares the same underlying idea as the SACOT-χ scheme in deeply-inelastic scattering [10].

Part of the $\log(p_{\mathrm{T}}^2/m^2)$ terms in FFNS come also from final-state splittings. As an example, Figure 2 shows a diagram in which an outgoing gluon splits into a $Q\overline{Q}$ pair. The result-

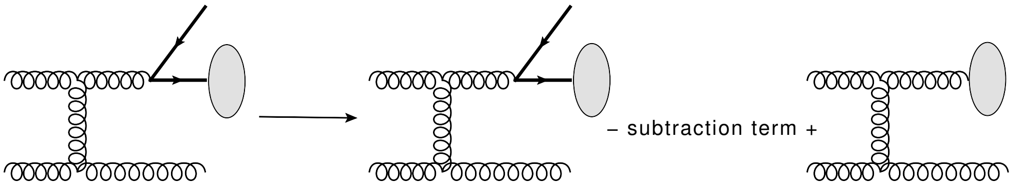

Figure 2: Origin of the gluon-fragmentation subprocess illustrated.

ing $\log(p_{\mathrm{T}}^2/m^2)$ terms are absorbed into the fragmentation-scale (μ_{frag}) dependent gluon FFs, $D_{g\to \mathrm{D}^0}(z,\mu^2_{\mathrm{frag}})$, giving rise to gluon-fragmentation contributions,

$$\int \frac{dz}{z} dx_1 dx_2\, f_g^p(x_1,\mu^2_{\mathrm{fact}}) \frac{d\hat{\sigma}^{gg\to g+X}(\tau_1,\tau_2)}{dp_{\mathrm{T}}dy} f_g^p(x_2,\mu^2_{\mathrm{fact}}) D_{g\to \mathrm{D}^0}(z,\mu^2_{\mathrm{frag}})\,.$$

The subtraction term avoiding the double counting is again the same expression, but replacing the gluon FF by its perturbative form,

$$D_{g\to \mathrm{D}^0}(x,\mu^2_{\mathrm{frag}}) = \left(\frac{\alpha_s}{2\pi}\right) \log\left(\frac{\mu^2_{\mathrm{frag}}}{m^2}\right) \int_x^1 \frac{\mathrm{d}\ell}{\ell} P_{qg}\left(\frac{x}{\ell}\right) D_{Q\to \mathrm{D}^0}(\ell) + \mathscr{O}(\alpha_s^2)\,.$$

In line with our scheme choice, the $\overline{\mathrm{MS}}$ zero-mass matrix elements for $d\hat{\sigma}^{gg\to g+X}(\tau_1,\tau_2)$ with the massive expressions for $\tau_{1,2}$, are adopted. Even if the heavy quarks do not explicitly appear in the $gg\to g+X$ process, the underlying process is also here the $Q\overline{Q}$-pair production.

With this schematic justification, our "master formula" within GM-VFNS is,

$$\frac{d\sigma^{pp\to \mathrm{D}^0+X}}{dP_{\mathrm{T}}dY} = \sum_{ijk} \int \frac{dz}{z} dx_1 dx_2 f_i^p(x_1,\mu^2_{\mathrm{fact}}) \frac{d\hat{\sigma}^{ij\to k}(\tau_1,\tau_2,m,\mu^2_{\mathrm{ren}},\mu^2_{\mathrm{fact}},\mu^2_{\mathrm{frag}})}{dp_{\mathrm{T}}dy} f_j^p(x_2,\mu^2_{\mathrm{fact}}) D_{k\to \mathrm{D}^0}(z,\mu^2_{\mathrm{frag}})\,. \tag{3.1}$$

Unlike in FFNS, all partonic subprocesses are included and the FFs are scale dependent. In the limit $p_{\mathrm{T}}\to 0$, the partonic cross sections reduce to FFNS, but towards $p_{\mathrm{T}}\to\infty$ they tend to the zero-mass $\overline{\mathrm{MS}}$ expressions. Our numerical realization of SACOT-m_{T} scheme is crafted around the Mangano-Nason-Ridolfi code [3] for heavy quarks, and the INCNLO code [11] for zero-mass partons. All terms up to $\mathscr{O}(\alpha_s^3)$ are included.

4. Description of the LHCb D^0 data

In Figure 3, we compare the LHCb 13 TeV D^0 data [12] with our GM-VFNS theory calculation. The darker bands show the NNPDF3.1 (pch) [13] PDF uncertainty, and the lighter bands combine the scale-variation and PDF errors. We have used here the KKKS08 FFs [14]. The calculation agrees very well with the data though the scale variation leads to a significant uncertainty at small P_{T}. We have found that, the contribution from the three FFNS processes, including the subtraction terms, is less than 10% for $P_{\mathrm{T}}\gtrsim 3\,\mathrm{GeV}$ and only around 3% for $P_{\mathrm{T}}\gtrsim 10\,\mathrm{GeV}$. This demonstrates that the $\log(p_{\mathrm{T}}^2/m^2)$ terms in FFNS become quickly the dominant ones and must be resummed as done in GM-VFNS. A comparison using FFNS + parton-shower approach (with the same PDFs) is also presented. Here, we have used the POWHEG-BOX event generator [5] matched to the PYTHIA 8 [15] parton shower. We see that the POWHEG+PYTHIA setup has a tendency to

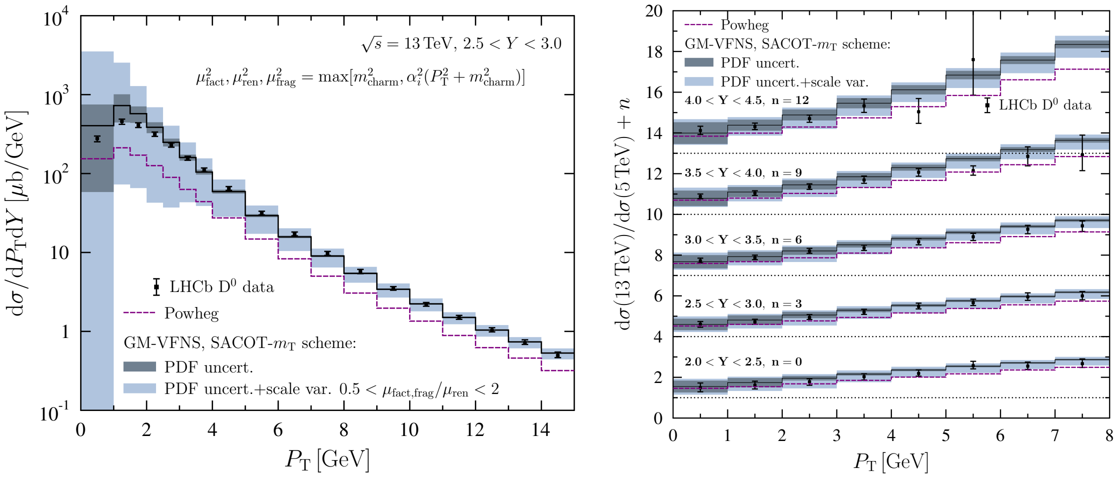

Figure 3: Left: LHCb D^0 data [12] in p-p collisions at $\sqrt{s} = 13\,\mathrm{TeV}$ compared to our GM-VFNS calculation and the POWHEG+PYTHIA framework. Right: Ratio between $\sqrt{s} = 13\,\mathrm{TeV}$ and $\sqrt{s} = 5\,\mathrm{TeV}$ data.

underpredict the experimental spectrum, and the ratio between two $\sqrt{s}$ is clearly flatter than the GM-VFNS prediction. We deduce that the leading reason is that by starting only with $c\bar{c}$ pairs (generated by POWHEG) one neglects the contributions in which the parton shower excites the $c\bar{c}$ pair only later on. In GM-VFNS these are resummed to the scale-dependent FFs and, indeed, e.g. the gluon-to-D contributions can be around 50% of the total budget. The gluon fragmentation also significantly changes the x regions in which the PDFs are sampled. Thus, the use of FFNS-based computation when using D-meson data to fit GM-VFNS PDFs would inflict a potential bias.

Acknowledgments

The support by the Academy of Finland Projects 297058 & 308301, the Carl Zeiss Foundation, and the state of Baden-Württemberg through bwHPC, are acknowledged. We have used the computing facilities of the Finnish IT Center for Science (CSC) in our work.

References

[1] O. Zenaiev *et al.*, Eur. Phys. J. C **75** (2015) 396.
[2] R. Gauld and J. Rojo, Phys. Rev. Lett. **118** (2017) 072001.
[3] M. L. Mangano, *et al.*, Nucl. Phys. B **373** (1992) 295.
[4] M. Cacciari, *et al.*, JHEP **9805** (1998) 007.
[5] S. Frixione, *et al.*, JHEP **0709** (2007) 126.
[6] I. Helenius and H. Paukkunen, JHEP **1805** (2018) 196.
[7] O. Zenaiev, Eur. Phys. J. C **77** (2017) no.3, 151.
[8] R. S. Thorne and W. K. Tung, arXiv:0809.0714 [hep-ph].
[9] B. A. Kniehl *et al.*, Phys. Rev. D **71** (2005) 014018.
[10] M. Guzzi, *et al.*, Phys. Rev. D **86** (2012) 053005.
[11] F. Aversa, *et al.*, Nucl. Phys. B **327** (1989) 105.
[12] R. Aaij *et al.*, JHEP **1603** (2016) 159.
[13] R. D. Ball *et al.*, Eur. Phys. J. C **77** (2017) 663.
[14] T. Kneesch, *et al.*, Nucl. Phys. B **799** (2008) 34.
[15] T. Sjöstrand *et al.*, Comput. Phys. Commun. **191** (2015) 159.